Available online at www.sciencedirect.com

ScienceDirect

www.elsevier.com/locate/jes

JES JOURNAL OF ENVIRONMENTAL SCIENCES

www.jesc.ac.cn

Effects of calcination temperature on physicochemical property and activity of $CuSO_4/TiO_2$ ammonia-selective catalytic reduction catalysts

Yanke Yu [1,2], *Jiali Zhang* [1,3], *Changwei Chen* [1], *Chi He* [1,4,*], *Jifa Miao* [5], *Huirong Li* [5], *Jinsheng Chen* [5,*]

[1] *Department of Environmental Science and Engineering, School of Energy and Power Engineering, Xi'an Jiaotong University, Xi'an 710049, China*

[2] *Department of Chemical Engineering, Columbia University, New York 10027, USA*

[3] *College of Geology and Environment, Xi'an University of Science and Technology, Xi'an 710054, China*

[4] *National Engineering Laboratory for VOCs Pollution Control Material and Technology, University of Chinese Academy of Sciences, Beijing 101408, China*

[5] *Center for Excellence in Regional Atmospheric Environment, Institute of Urban Environment, Chinese Academy of Sciences, Xiamen 361021, China*

ARTICLE INFO

Article history:
Received 3 September 2019
Received in revised form
13 January 2020
Accepted 13 January 2020
Available online 24 January 2020

Keywords:
Calcination temperature
Sulfate catalyst
Selective catalytic reduction of nitrogen oxides by NH_3
Surface acidity
NH_3 oxidation

ABSTRACT

$CuSO_4/TiO_2$ catalysts with high catalytic activity and excellent resistant to SO_2 and H_2O, were thought to be promising catalysts used in Selective catalytic reduction of nitrogen oxides by NH_3. The performance of catalysts is largely affected by calcination temperature. Here, effects of calcination temperature on physicochemical property and catalytic activity of $CuSO_4/TiO_2$ catalysts were investigated in depth. Catalyst samples calcined at different temperatures were prepared first and then physicochemical properties of the catalyst were characterized by N_2 adsorption-desorption, X-ray diffraction, thermogravimetric analysis, Raman spectra, Fourier-transform infrared spectroscopy, X-ray photoelectron spectroscopy, temperature-programmed desorption of NH_3, temperature-programmed reduction of H_2 and in situ diffuse reflectance infrared Fourier transform spectroscopy. Results revealed that high calcination temperature had three main effects on the catalyst. First, sintering and anatase transform into rutile with increase of calcination temperature, causing a decrement of specific surface area. Second, decomposition of $CuSO_4$ under higher calcination temperature, resulting in disappears of Brønsted acid sites (S—OH), which had an adverse effect on surface acidity. Third, CuO from the decomposition of $CuSO_4$ changed surface reducibility of the catalyst and favored the process of NH_3 oxidation to nitrogen oxides (NO_x). Thus, catalytic activity of the catalyst calcined under high temperatures (≥600°C) decreased largely.

* *Corresponding authors.*
E-mail addresses: chi_he@xjtu.edu.cn (C. He), jschen@iue.ac.cn (J. Chen).

https://doi.org/10.1016/j.jes.2020.01.010

Introduction

As an efficient method to abate nitrogen oxides (NO_x) from the combustion of fossil fuels, selective catalytic reduction of NO_x by NH_3 (NH_3-SCR) over catalysts have attracted much attention (Odenbrand, 2018; Chen et al., 2018b). Due to high NO_x removal efficiency and excellent SO_2 tolerance, vanadium-based catalysts are the main commercial SCR catalysts used today (He et al., 2018; Chen et al., 2018a). However, some shortcomings of vanadium-based catalysts such as biological toxicity of vanadium and undesirable activity of SO_2 oxidation still existed (Wang et al., 2019; Yu et al., 2019b). Thus, novel vanadium-free SCR catalysts are developed by many researchers (Yan et al., 2019; Cheng et al., 2019; Lian et al., 2019; Woo et al., 2019). Metal oxides and zeolite catalysts performed high activity in NH_3-SCR reaction, but their low SO_2 tolerance has been one of main obstacles for industrial applications (Gao et al., 2017; Hammershøi et al., 2018; Wijayanti et al., 2016).

From the view point of high SO_2 tolerance, metal sulfates were used in NH_3-SCR reaction by some researchers (Ma et al., 2011; Du et al., 2016; Yu et al., 2017). $Fe_2(SO_4)_3/TiO_2$ catalysts performed high activity with NO_x conversion higher than 90% in temperature range from 350 to 450°C; moreover, they owned a high resistant to water and SO_2 (Ma et al., 2011). Support $Fe_2(SO_4)_3$ and $CuSO_4$ on Ce–Ti mixed oxides catalysts displayed higher activity than vanadium-based catalysts in the temperature range from 250 to 350°C, in addition, the support metal sulfate catalysts also showed high resistances to SO_2 (Du et al., 2016). In our previous work, due to abundant acid sites (both Brønsted and Lewis acid sites) on catalyst surface, we found that $CuSO_4/TiO_2$ catalysts with 10 wt.% $CuSO_4$ performed high NH_3-SCR activity in temperature range from 280 to 380°C and the catalysts owned excellent tolerance to water and SO_2 (Yu et al., 2017). Metal sulfate catalysts have been thought to be promising SCR catalysts used in industry. However, compared with metal oxides and zeolite catalysts, the researches about metal sulfate catalysts are less and more attention should be paid.

Calcination temperature is an important factor for preparing catalysts. The calcination temperature can affect physicochemical properties of SCR catalysts, such as distribution of active sites, surface acidity and reducibility, thus impact the catalytic performance largely (Wu et al., 2016, 2019). The effects of calcination temperature on physicochemical properties and catalytic activity of $CuSO_4/TiO_2$ catalysts are still unknown.

In this work, $CuSO_4/TiO_2$ catalysts were calcined at 500, 600 and 700°C, respectively. The effects of calcination temperature on physicochemical properties of the catalyst were investigated in depth by N_2 adsorption-desorption, X-ray diffraction (XRD), thermogravimetric analysis (TGA), Raman spectra, Fourier-transform infrared spectroscopy (FTIR), X-ray photoelectron spectroscopy (XPS), temperature-programmed desorption of NH_3 (NH_3-TPD), temperature-programmed reduction of H_2 (H_2-TPR) and in situ diffuse reflectance infrared Fourier transform spectroscopy (in situ DRIFTS). The NH_3-SCR activity of all prepared catalysts was also tested.

1. Materials and methods

1.1. Catalysts preparation

TiO_2 (anatase, Aladdin Industrial Corporation, USA) (6.0 g) was mixed with 1.04 g of $CuSO_4 \cdot 5H_2O$ (analytical reagent, Sinopharm Chemical Reagent Corporation, China) in an agate mortar and grinded to uniformity. Then mixed powder was calcined at 500°C in air for 5 hr (named CuSTi). In order to determine the effect of calcination temperature on the catalyst, 2.0 g of CuSTi sample was calcined at 600 and 700°C in air for 3 hr, named CuSTi-600 and CuSTi-700, respectively.

1.2. Activity test

The catalytic activity of the sample was tested on a fixed-bed quartz reactor (diameter 10 mm and height 600 mm). Catalyst sample (1.0 mL, 20–40 mesh) was placed in middle of the reactor. The mixture gas contained 700 ppmV NO, 700 ppmV NH_3, 5.0 vol.% H_2O and 4.0 vol.% O_2 in N_2. Total gas flow rate was 1000 mL/min, corresponding to gas hourly space velocity (GHSV) = 60,000 hr^{-1}. Concentrations of NO, NO_2, N_2O and NH_3 in the gas were detected by a Fourier transform infrared spectrometer (FTIR) gas analyzer (IGS, Thermo Fisher, USA). NO_x conversion (x) was calculated from Eq. (1):

$$x = \frac{C_{NO_x,in} - C_{NO_x,out}}{C_{NO_x,in}} \times 100\% \quad (1)$$

where, $C_{NOx,in}$ and $C_{NOx,out}$ mean the concentration of NO_x ($NO + NO_2$) in the inlet and outlet, respectively.

The oxidation of NH_3 by O_2 over each catalyst sample was also tested (the mixture gas contained 700 ppmV NH_3, 5.0 vol.% H_2O and 4.0% O_2 in N_2) and the conversion of NH_3 to NO_x (y) under NH_3 oxidation conditions was calculated from Eq. (2):

$$y = \frac{C_{NO_x,out}}{C_{NH_3,in}} \times 100\% \quad (2)$$

where $C_{NH3,in}$ means the concentration of NH_3 in the inlet and $C_{NOx,out}$ means the concentration of NO_x ($NO + NO_2$) in the outlet under NH_3 oxidation conditions.

1.3. Catalyst characterizations

N_2 adsorption-desorption isotherm of the catalyst sample was recorded by a surface area and pore size analyzer (NOVA, 2000e; Quantachrome Company, USA). Powder XRD of each sample was carried out on X'Pert Pro XRD diffractometer (EPSILON5, PANalytical B.V., Netherland), using Cu palladium and $K\alpha$ radiation. The mean crystallite size of anatase (d_{crys}) was calculated by Scherrer Eq. (3) based on full width at half maximum (FWHM) of the (101) plane.

$$d_{crys} = \frac{K\lambda}{\sigma\cos\theta} \quad (3)$$

where K is a constant which depends on the catalyst particles and is generally assumed to be 1, λ is the wavelength of the X-ray radiation, σ is the full width at half maxima (FWHM) of (101) plane, and θ is the position of (101) plane.

TGA was collected on an HCT-1 thermo analyzer (HCT-1, Beijing Hengjiu Company, China) under an air flowing (20 mL/min). Laser Raman spectra were collected on laser Raman spectrometer (LabRAM Aramis, HORIBA Jobin Yvon, France) with Ar ion laser (514.5 nm). FTIR was recorded on Bruker Vertex 70 infrared spectrometer (Vertex 70, Bruker Corporation, Germany), 4 cm^{-1} (32 scans). XPS was recorded on ESCALAB 250 spectrometer (ESCALAB 250, Thermo Fisher Scientific Company, USA) with Al Kα radiation. H_2-TPR of the sample was recorded on ChemBET-3000 TPR-TPD chemisorption analyzer (ChemBET-3000, Quantachrome, USA) and an online mass spectrum (MS, DYCOR LC-D100, Ametek Company, USA) was used to record the concentration of H_2 ($m/z = 2$) and SO_2 ($m/z = 64$). NH_3-TPD was also recorded on the ChemBET-3000 TPR-TPD chemisorption analyzer. The signal of NH_3 ($m/z = 16$) was recorded by online MS.

In situ DRIFTS was performed on Bruker Vertex 70 infrared spectrometer (Vertex 70, Bruker Corporation, Germany) with mercury-cadmium-telluride (MCT) detector. Powder sample in the reaction cell (Horizon, Harrick Scientific, USA) was treated under N_2 at 450°C for 1 hr to remove the surface impurities. Then reaction cell was cooled to 300°C. Background spectrum was recorded. Afterwards, 2000 ppmV NH_3/N_2 was inlet to the reaction cell for 15 min and then purged with N_2 for another 15 min.

2. Results and discussion

2.1. Physicochemical property of materials

The specific surface area (S_{BET}), total pore volume (V_p) and average pore diameter (D_p) of the catalyst calcined at different temperature are shown in Table 1. S_{BET} of CuSTi sample calcined at 500°C was 46.2 m^2/g with V_p of 0.257 cm^3/g and D_p of 11.1 nm. When the calcination temperature increased to 600°C, S_{BET} and V_p of CuSTi-600 sample decreased to 29.0 m^2/g and 0.212 cm^3/g, about 63% and 82% of CuSTi sample. Meanwhile, D_p of CuSTi-600 sample increased to 14.6 nm. The calcination temperature of 700°C had a significantly negative effect on the pore structure of the catalyst. S_{BET} of CuSTi-700 sample decreased sharply to 4.6 m^2/g, only 10% of CuTiS sample and V_p decreased to 0.062, about 24% of CuTiS sample. However, D_p of CuSTi-700 sample increased to 27.1 nm, 2.4 times of CuSTi sample. It could be concluded that higher calcination temperature could destroy the pore structure of catalysts and lead to the sharply decrease of specific surface area. The low surface area would result in decrement of active sites, which was harmful to catalytic activity.

Table 1 – Textural property of the catalyst sample.

Sample	S_{BET} (m^2/g)	V_p (cm^3/g)	D_p (nm)	T_{acid} (mmol/g)
CuSTi	46.2	0.257	11.1	3.65
CuSTi-600	29.0	0.212	14.6	1.50
CuSTi-700	4.6	0.062	27.1	/

S_{BET}: specific surface area obtained at relative pressure (P/P_0) = 0.05–0.30; V_p: total pore volume obtained at $P/P_0 = 0.99$; D_p: Barrett-Joyner-Halenda (BJH) pore diameter calculated from the N_2 desorption branch; T_{acid}: total amount of acid sites calculated by the integral area of NH_3 desorption peak from temperature-programmed desorption of NH_3 (NH_3-TPD). CuSTi, CuSTi-600 and CuSTi-700 refer to fresh catalyst, catalysts calcined at 600°C and catalysts calcined at 700°C, respectively.

The effects of calcination temperature on crystal structure of the catalyst are shown in Fig. 1. Diffraction peaks assigned to anatase TiO_2 could be found on CuSTi sample. Besides, a small peak at $2\theta = 34.3°$ which was assigned to $CuSO_4$ appeared, suggesting that $CuSO_4$ had a good dispersion on the carrier. The results of scanning transmission electron microscope (STEM)-mapping (Appendix A Fig. S1) also indicated that $CuSO_4$ had a good dispersion. As shown in Appendix A Fig. S1, S elements presented a good dispersion on the catalyst surface. After the calcination temperature reached 600°C, CuSTi-600 sample still showed diffraction peaks of anatase, but intensities of the peaks increased. According to Scherrer Equation, mean crystallite size (d_{crys}, based on FWHM of the peak at $2\theta = 25.3°$) of anatase for CuSTi sample was 21.8 nm, similar to other researches (Miszczak and Pietrzyk, 2015). However, d_{crys} of CuSTi-600 sample increased to 26.5 nm, suggesting that calcined at 600°C caused sintering of the carrier. The small peak assigned to $CuSO_4$ disappeared on CuSTi-600 sample, implying that part of $CuSO_4$ decomposed. After the catalyst was calcined at 700°C, the diffraction peaks changed significantly. Though the diffraction peaks assigned to anatase could be detected, intensities of the peaks decreased largely. Diffraction peaks of rutile were clear on CuSTi-700 sample, suggesting that rutile was the main crystal form of TiO_2. Among the crystal forms of TiO_2, anatase was not thermodynamically stable and would transform into rutile under high temperature (Miszczak and Pietrzyk, 2015). There were no peaks assigned to $CuSO_4$ and new peaks at $2\theta = 35.5°$ and 48.7° which could be associated with CuO appeared, implying that $CuSO_4$ totally decomposed (Eq. (4)). The TGA results of $CuSO_4/TiO_2$ catalysts also prove this conclusion. As shown in Appendix A Fig. S2, the loss of mass start from 580°C and end at 790°C with a mass loss of 4.8%, which could be associated with decomposition of $CuSO_4$ on the sample (the theoretical

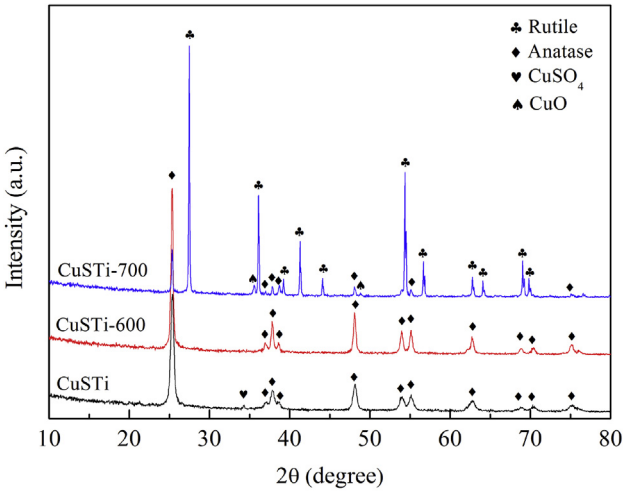

Fig. 1 – X-ray diffraction (XRD) of the catalyst calcined at different temperatures.

value was 5.0%). High calcination temperature would cause the sintering and anatase-to-rutile transformation of the carrier, destroying the pore structure of the catalyst, thus led to significant decrease of specific surface area.

$$CuSO_4 \rightarrow CuO + O_2 + SO_2 \quad (4)$$

The influence of calcination temperature on morphology of the catalyst was investigated by SEM and the photos are shown in Fig. 2. The particles on $CuSO_4/TiO_2$ catalyst calcined at 500°C were sphere shape with uniform size and presented a good distribution. When the calcination temperature increased to 600°C, it could be found that agglomeration appeared and the size of the sphere particles increased largely, indicating that sintering of the catalyst should occur, in accordance with the result of XRD. The agglomeration and accumulation were more serious on CuSTi-700 sample and the particles were inhomogeneous, which could destroy the pore structure and cause the decrease of surface area and pore volume. Moreover, the serious agglomeration and accumulation of surface particles would hinder the mass transfer and diffusion of reactant and product gases (Xu et al., 2018; Zhao et al., 2018), which could lead to the decrease of catalytic activity.

Raman spectra of catalysts after normalization are shown in Fig. 3. CuSTi sample showed three main peaks at 391, 515, and 636 cm^{-1} and a small peak at 792 cm^{-1}, which were the typical Raman peaks of TiO_2 (Yao et al., 2017; Ceballos-Chuc et al., 2018). CuSTi sample also presented another small peak at 1094 cm^{-1}, which could be assigned to ν_{asym} (SO) of sulfates (Ramis et al., 1996). The peaks assigned to TiO_2 didn't change after the calcination temperature increased to 600°C. However, the peak at 1094 cm^{-1} assigned to sulfate was almost disappear, implying part of sulfates decomposed at 600°C, consistent with the results of XRD and TGA. After $CuSO_4/TiO_2$ was calcined at 700°C, the peaks assigned to TiO_2 changed remarkably, suggesting high temperature had a large influence on the carrier, and the anatase-to-rutile transformation should occur (Nova et al., 2001). FTIR was also used to investigate the influence of calcination temperature on $CuSO_4/TiO_2$ catalyst and the results are presented in Appendix A Fig. S3. A broad peak in the range from 900 to 400 cm^{-1} on CuSTi sample could be assigned to anatase TiO_2 (Yu et al., 2019a). The peaks at 981, 1062, 1141 cm^{-1} and a shoulder peak at 1220 cm^{-1} could be assigned to surface sulfate and bisulfate (Yu et al., 2019a). With the increase of calcination temperature, the broad peak assigned to anatase TiO_2 split into two peaks, suggesting that sintering and the anatase-to-rutile transformation of TiO_2 occurred. The intensity of peaks at 981, 1062, 1141 and 1220 cm^{-1} decreased significantly with the increase of calcination temperature, indicating sulfate and bisulfate would decompose under high temperature. From the results of Raman, FTIR and XRD, it could be concluded that higher calcination temperature could cause the decomposition of $CuSO_4$, sintering and the anatase-to-rutile transformation of TiO_2.

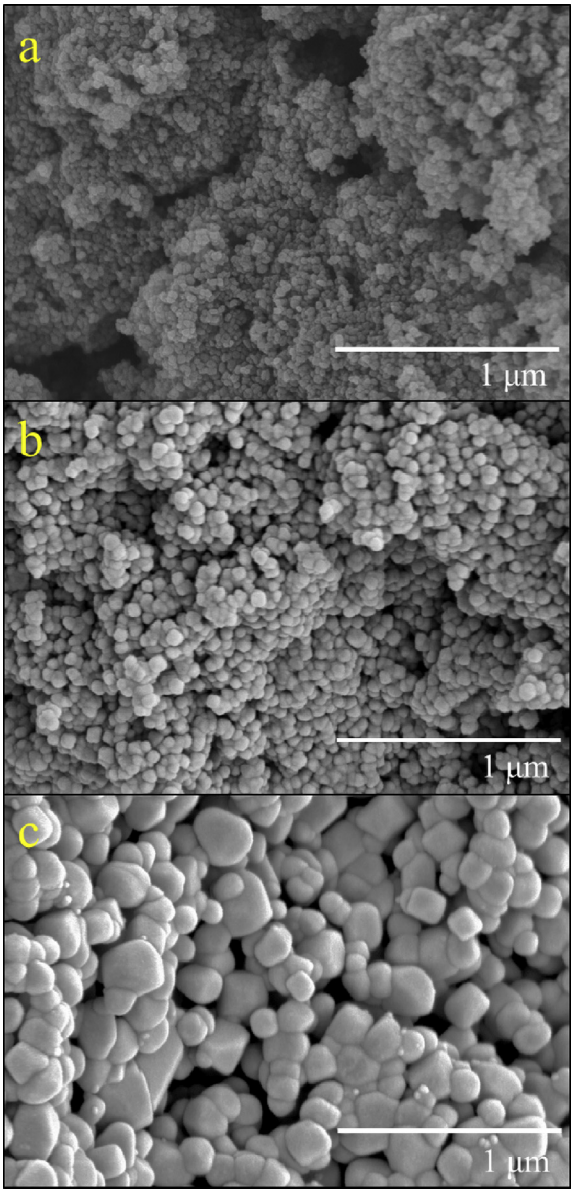

Fig. 2 – Scanning electron microscope (SEM) photos of the (a) CuSTi, (b) CuSTi-600 and (c) CuSTi-700 catalysts.

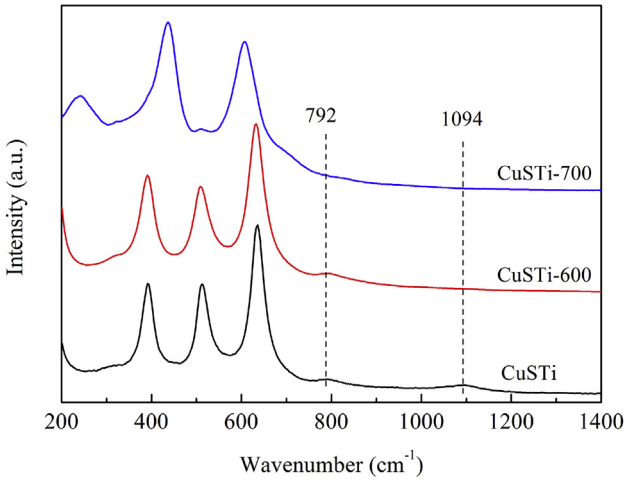

Fig. 3 – Raman spectra of the catalyst calcined at different temperatures.

XPS spectra of S 2p and O 1s for the catalyst calcined at different temperatures are presented in Fig. 4. On CuSTi sample, three peaks centered at 166.5, 168.6 and 170.0 eV were found, which could be assigned to sulfite, sulfate and bisulfate, respectively (Yang et al., 2011; Huang et al., 2014). When the calcination temperature increased to 600°C, it could be found that the peak assigned to sulfite disappeared, suggesting that sulfite on the catalyst should decompose. No peaks assigned to sulfite or sulfate on CuSTi-700 sample could be found, implying that all $CuSO_4$ decomposed after calcined at 700°C, in accordance with the results of XRD and Raman spectra. There were three O species on CuSTi sample (Table 2), which were lattice oxygen (O_α, 530.0 eV), surface OH group (O_β, 531.6 eV) and adsorbed oxygen (O_γ, 533.4 eV) (Yu et al., 2017; Jian et al., 2019). After the catalyst calcined at 600°C, the concentration of surface OH group decreased from 45.1% to 35.0%. The concentration of surface OH group was only 16.1% on CuSTi-700 sample. It could be concluded that high calcination temperature would reduce the concentration of surface OH group on the catalyst. According to previous researches, metal sulfate could form S–OH on the catalyst surface. The decomposition of metal sulfate should be one of the main reasons for the concentration decrease of surface OH group. Because surface OH group could act as Brønsted acid sites (Yu et al., 2017), the high calcination temperature should damage the Brønsted acid sites of the catalyst.

Acid sites play an important role in NH_3-SCR reaction (Zha et al., 2018). NH_3-TPD was used to characterize the acid sites of each sample and the results can be found in Fig. 5. CuSTi sample presented three peaks at 175, 261 and 321°C, which should be assigned to weak, medium and strong acid sites, respectively. According to the amount of NH_3 desorption during NH_3-TPD experiment, the total amount of acid sites (T_{acid}) was calculated and it was 3.65 mmol/g for CuSTi sample. When the calcination temperature increased to 600°C, it could be found that the amount of NH_3 desorption decreased largely and T_{acid} was 1.50 mmol/g, about 41% of CuSTi sample. There was little amount of NH_3 desorption on CuSTi-700 sample, suggesting that the acid sites almost disappeared after the catalyst calcined at 700°C. High calcination temperature would cause decomposition of $CuSO_4$ and the decrease of specific surface area, which should be the main reason for the amount decrease of acid sites.

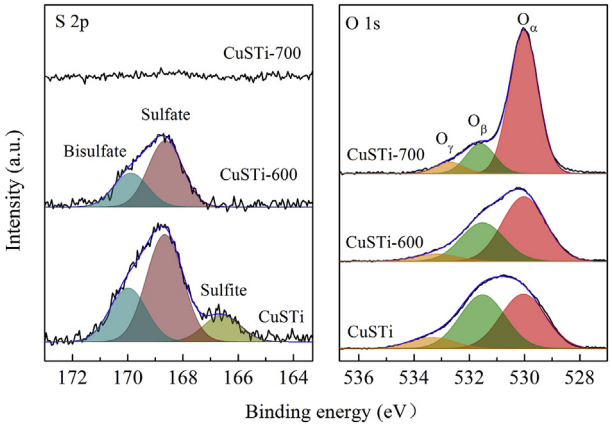

Fig. 4 – S 2p and O 1s X-ray photoelectron spectroscopy (XPS) spectra of the prepared catalysts. O_α: lattice oxygen; O_β: surface OH group; O_γ: adsorbed oxygen.

Table 2 – Content of oxygen species in synthesized catalysts (%).

Sample	O_α	O_β	O_γ
CuSTi	45.6 (530.1)	45.1 (531.6)	9.3 (533.4)
CuSTi-600	58.5 (530.1)	35.0 (531.6)	6.5 (533.3)
CuSTi-700	77.6 (530.1)	16.1 (531.7)	6.3 (532.8)

Data in parentheses means the position of XPS peak (eV).

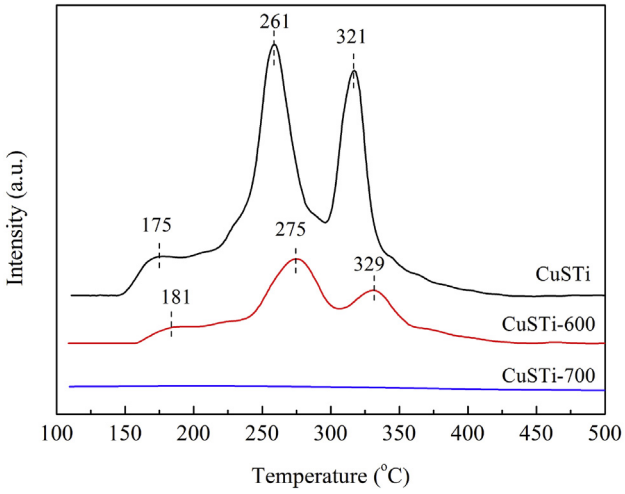

Fig. 5 – Temperature-programmed desorption of NH_3 (NH_3-TPD) results of the prepared catalysts.

The surface reducibility of catalyst has a significant effect on NH_3-SCR reaction (Cao et al., 2019; Leistner et al., 2018). The effect of calcination temperature on the surface reducibility was characterized by H_2-TPR and the results are shown in Fig. 6a. In addition, the emission of SO_2 during H_2-TPR experiment was detected by MS and the results can be found in Fig. 6b. H_2 consumption started from 250°C and ended at 550°C on CuSTi sample. The signal of SO_2 was almost parallel to H_2 consumption. Compared with CuSTi sample, H_2 consumption of CuSTi-600 sample at low temperature decreased obviously, but the signal at high temperature was similar to CuSTi sample. The signal of SO_2 also presented the same trend, implying part of sulfate and sulfite decomposed when the catalyst calcined at 600°C, consistent with the results of XPS. However, the H_2 consumption of CuSTi-700 was significantly different from CuSTi sample and there was no signal of SO_2 during H_2-TPR process. All $CuSO_4$ in the catalyst should decompose into CuO and the formation of CuO caused the change of surface reducibility on the catalyst calcined at 700°C.

The results for in situ DRIFTS of NH_3 over each sample under 300°C are shown in Fig. 7. Several bonds at 1319, 1388, 1442, 1601, 3182, 3280, 3351 cm^{-1} and a wide band from 1645 to 1855 cm^{-1} were found on $CuSO_4/TiO_2$ catalysts. The bond at 1442 cm^{-1} and the wide band from 1645 to 1855 cm^{-1} could be assigned to NH_4^+ on Brønsted acid sites (B) (Yu et al., 2017; Ye

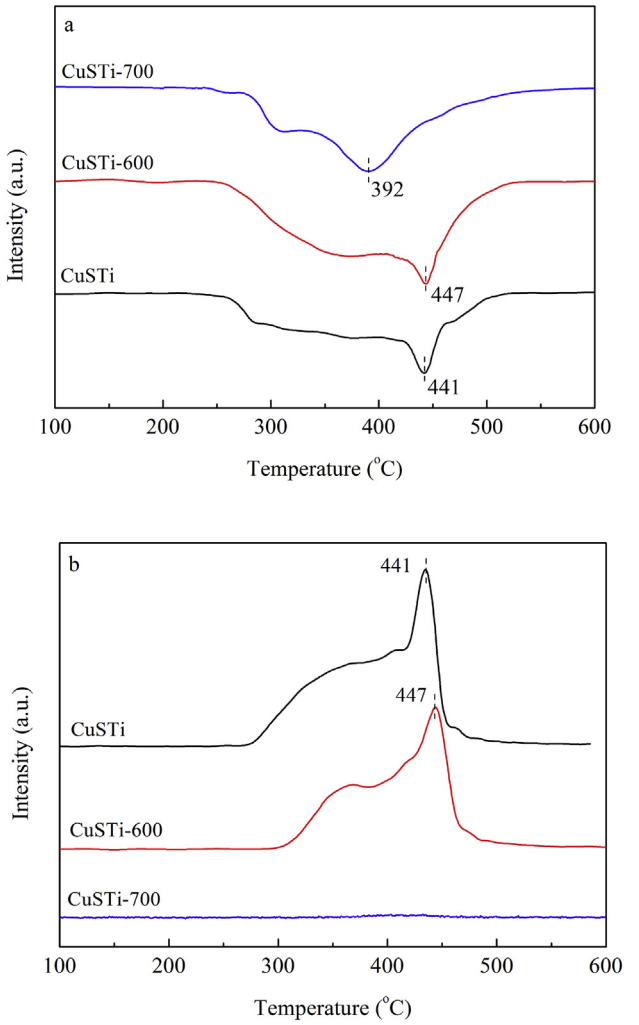

Fig. 6 – (a) Temperature-programmed reduction of H_2 (H_2-TPR) of the catalyst calcined at different temperatures and (b) emission of SO_2 during H_2-TPR process.

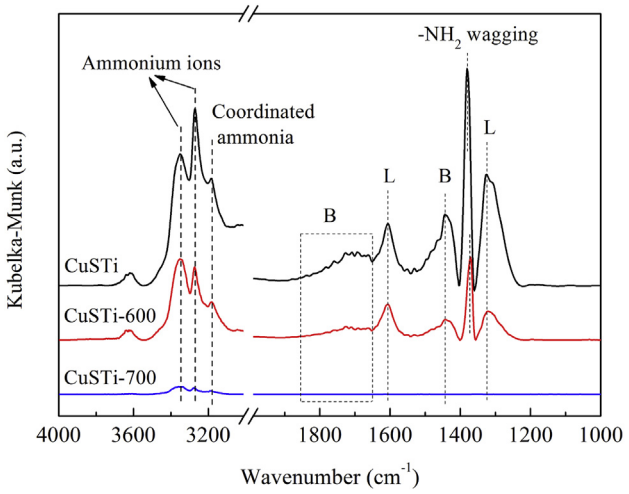

Fig. 7 – In situ diffuse reflectance infrared Fourier transform spectroscopy (DRIFTS) of NH_3 on CuSTi, CuSTi-600 and CuSTi-700 sample at 300°C. B: Brønsted acid sites; L: Lewis acid sites.

et al., 2019). Meanwhile, the bonds at 1319 and 1601 cm^{-1} could be assigned to NH_3 on Lewis acid sites (L) (Yu et al., 2017; Ye et al., 2019). Our previous work indicated that both Brønsted and Lewis acid sites participated in NH_3-SCR reaction (Yu et al., 2017). At high wavenumbers, the band at 3182 cm^{-1} could be attributed to N–H of the coordinated ammonia on the catalyst surface and the bands at 3280 and 3351 cm^{-1} could be attributed to ammonium ions (Ma et al., 2014; Fan et al., 2018). After the catalyst was calcined at 600°C, it could be found that the intensity of the bonds assigned to Brønsted and Lewis acid sites decreased largely, suggesting that the amount of acid sites reduced, in accordance with the results of NH_3-TPD. The decrease of specific surface area and the decomposition of sulfite or sulfate should be the main reasons for the reduction of acid sites. The amount ratio of Brønsted to Lewis acid sites on the sample was calculated by the ratio of the peak intensity at 1442 cm^{-1} to the peak intensity at 1601 cm^{-1}. The ratio was 1.10 for CuSTi sample and 0.59 for CuSTi-600 sample, suggesting that the influence of calcination temperature on Brønsted acid sites was larger than Lewis acid sites. The decomposition of sulfite or sulfate at high calcination temperature would decrease the amount of surface S–OH, which was the main Brønsted acid sites on sulfate catalyst (Yu et al., 2017). When the calcination temperature increased to 700°C, almost all bonds disappeared, suggesting that high calcination temperature would destroy the acid sites on the catalyst, in accordance with the results of NH_3-TPD. The decomposition of $CuSO_4$ and the anatase transform into rutile should be the main reasons for the disappears of acid sites.

2.2. *Catalytic activity*

Fig. 8a presents NO_x conversion of the catalyst calcined at different temperatures. N_2 selectivity was also calculated and the result can be found in the insert of Fig. 8a. CuSTi sample performed high activity during 280–380°C with NO_x conversion higher than 90% and N_2 selectivity was more than 99% during 280–380°C. After calcined at 600°C, the NO_x conversion of CuSTi-600 sample decreased significantly at temperature higher than 340°C, suggesting that the calcination temperature of 600°C could impact catalytic activity to a certain extent. However, when the calcination temperature reached 700°C, the activity of CuSTi-700 sample decreased sharply and NO_x conversion even dropped to a negative value at 420°C. In addition, N_2 selectivity decreased from 94.6% to 59.1% at 420°C, suggesting that high calcination temperature would have a negative effect on N_2 selectivity of the catalyst.

The negative value of NO_x conversion for CuSTi-700 sample at 420°C should mean that NH_3 was oxidized to NO_x by O_2 over the sample. In order to confirm this conclusion, the oxidation of NH_3 by O_2 over each sample was tested and the results can be found in Fig. 8b. It could be found that the calcination temperature had a large effect on NH_3 conversion over the catalyst. The oxidation of NH_3 over CuSTi sample under the temperature lower than 380°C was hard to occur and the NH_3 conversion was only 4.1% at 420°C. When the calcination temperature increased to 600°C, the NH_3 conversion at

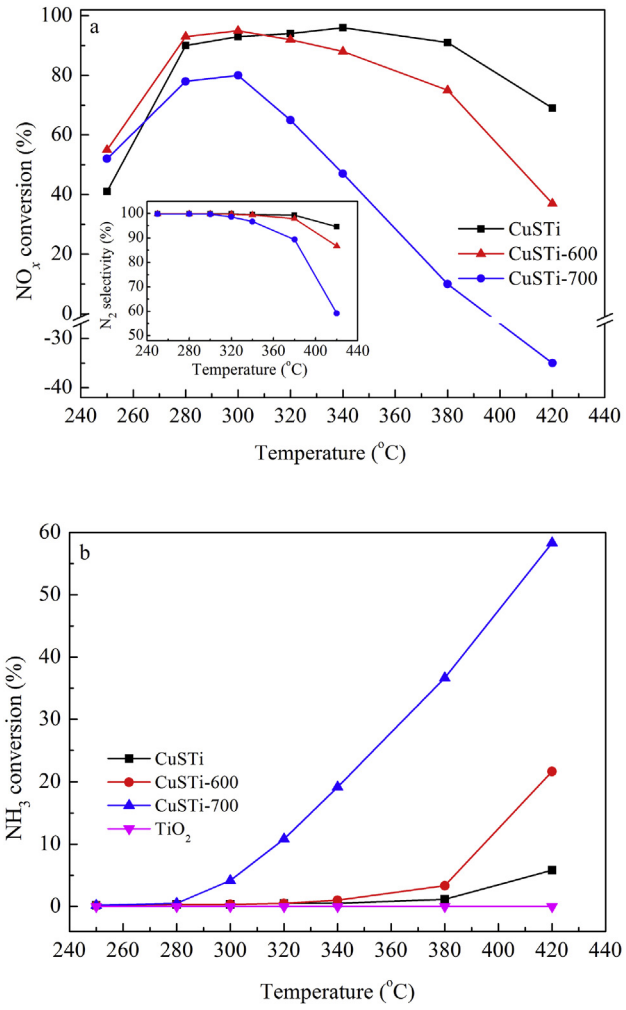

Fig. 8 – (a) NO_x conversion and (inset) N_2 selectivity of each sample and (b) NH_3 conversion over the catalyst under NH_3 oxidation conditions. Reaction conditions: 700 ppmV NO (absent for (b)), 700 ppmV NH_3, 5.0 vol.% H_2O and 4.0 vol.% O_2 in N_2, gas hourly space velocity 60,000 hr^{-1}.

temperature higher than 340°C increased significantly. After the catalyst was calcined at 700°C, it could be found that the NH_3 conversion increased sharply with temperature and reached 58.7% at 420°C. The oxidation of NH_3 on pure TiO_2 calcined at 700°C was also tested and the result can be found in Fig. 8b. It could be found that there was little NH_3 oxidized to NO_x on pure TiO_2. Thus, it can be concluded that NH_3 should be oxidized by O_2 over CuO of CuSTi-700 sample in NH_3-SCR reaction process and formed new NO_x at high temperature, which caused the sharply decrease of NO_x conversion (Scheme 1). According to other researches, Brønsted acid sites were not necessary for ammonia oxidation and Lewis acid sites were active for ammonia oxidation to nitrogen oxides (Si et al., 2010; Yu et al., 2014). The possible reaction routes for ammonia oxidation on Lewis acid sites are presented below.

$$NH_3(g) + \text{Lewis acid sites} \rightarrow NH_3(ads) \quad (5)$$

$$NH_3(ads) \rightarrow NH_2(ads) + H^+ + e^- \quad (6)$$

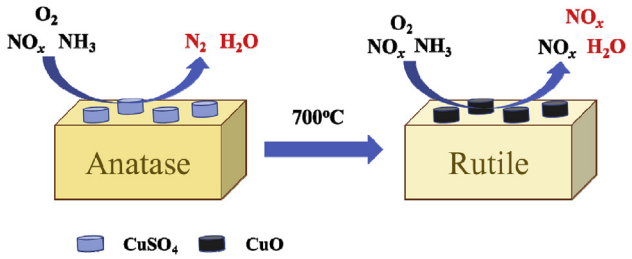

Scheme 1 – NH_3-selective catalytic reduction reaction over the catalyst calcined at different temperatures.

$$2NH_2(ads) + O(ads) \rightarrow 2NH(ads) + H_2O \quad (7)$$

$$NH(ads) + O(ads) \rightarrow HNO(ads) \quad (8)$$

$$2HNO(ads) + O(ads) \rightarrow H_2O + 2NO \quad (9)$$

where (g) and (ads) refer to gaseous phase and adsorption state, respectively.

As shown in Fig. 7, with the increase of calcination temperature, the amount of Brønsted acid sites decreased largely due to the decomposition of $CuSO_4$. Thus, the ammonia oxidation activity of the catalyst calcined at high temperature should be increased and considerable ammonia can't participate in NH_3-SCR reaction, which caused a decrease of NO_x conversion.

3. Conclusions

The calcination temperature had a large effect on physicochemical properties and activity of $CuSO_4/TiO_2$ catalysts. Higher calcination temperature would cause sintering and the anatase transform into rutile, which destroyed the pore structure and thus largely decreased the specific surface area. The decomposition of $CuSO_4$ under high calcination temperature led to the decrease of Brønsted acid sites amount and had an adverse effect on surface acidity, which could cause the decrease of catalytic activity. Moreover, CuO from the decomposition of $CuSO_4$ under higher calcination temperature favored the oxidation of NH_3, causing the significant decrease of SCR activity.

Conflict of interest

The authors declared that they have no conflicts of interest to this work.

Acknowledgments

This work was supported by the National Natural Science Foundation of China (Nos. 21906127, 21677114, 21876139 and 21922606), the Key R&D Program of Shaanxi Province (Nos. 2019SF-244 and 2019ZDLSF05-05-02), the China Postdoctoral

Science Foundation (No. 2016M602831), Natural Science Foundation of Shaanxi Province, China (No. 2019JQ-502) and the Fundamental Research Funds for the Central Universities (Nos. xjj2017113 and xjj2017170). Dr. Yanke Yu also acknowledges financial supports from the China Scholarship Council and the authors gratefully acknowledge the support of K.C. Wong Education Foundation.

Appendix A. Supplementary data

Supplementary data to this article can be found online at https://doi.org/10.1016/j.jes.2020.01.010.

REFERENCES

Cao, L., Wu, X.D., Xu, Y.F., Lin, Q.W., Hu, J.F., Chen, Y., et al., 2019. Ceria-modified WO_3-TiO_2-SiO_2 monolithic catalyst for high-temperature NH_3-SCR. Catal. Commun. 120, 55–58.

Ceballos-Chuc, M.C., Ramos-Castillo, C.M., Alvarado-Gil, J.J., Oskam, G., Rodríguez-Gattorno, G., 2018. Influence of brookite impurities on the Raman spectrum of TiO_2 anatase nanocrystals. J Phys. Chem. C 122, 19921–19930.

Chen, C.M., Gao, Y., Liu, S.T., Chen, J.M., Jia, W.B., 2018a. Review on the latest developments in modified vanadium-titanium-based SCR catalysts. Chin. J. Catal. 39, 1347–1365.

Chen, Y.X., Li, C., Chen, J.X., Tang, X.F., 2018b. Self-prevention of well-defined-facet Fe_2O_3/MoO_3 against deposition of ammonium bisulfate in low-temperature NH_3-SCR. Environ. Sci. Technol. 52, 11796–11802.

Cheng, J., Ye, Q., Zheng, C.K., Cheng, S.Y., Kang, T.F., Dai, H.X., 2019. Effect of ceria loading on Zr-pillared clay catalysts for selective catalytic reduction of NO with NH_3. New J. Chem. 43, 10850–10858.

Du, X.S., Wang, X.M., Chen, Y.R., Gao, X., Zhang, L., 2016. Supported metal sulfates on Ce-TiO_x as catalysts for NH_3-SCR of NO: High resistances to SO_2 and potassium. J. Ind. Eng. Chem. 36, 271–278.

Fan, J., Ning, P., Song, Z.X., Liu, X., Wang, L.Y., Wang, J., et al., 2018. Mechanistic aspects of NH_3-SCR reaction over CeO_2/TiO_2-ZrO_2-SO_4^{2-} catalyst: In situ DRIFTS investigation. Chem. Eng. J. 334, 855–863.

Gao, F.Y., Tang, X.L., Yi, H.H., Li, J.Y., Zhao, S.Z., Wang, J.G., et al., 2017. Promotional mechanisms of activity and SO_2 tolerance of Co- or Ni-doped MnO_x-CeO_2 catalysts for SCR of NO_x with NH_3 at low temperature. Chem. Eng. J 317, 20–31.

Hammershøi, P.S., Jensen, A.D., Janssens, T.V.W., 2018. Impact of SO_2-poisoning over the lifetime of a Cu-CHA catalyst for NH_3-SCR. Appl. Catal. B-Environ. 238, 104–110.

He, G.Z., Lian, Z.H., Yu, Y.B., Yang, Y., Liu, K., Shi, X.Y., et al., 2018. Polymeric vanadyl species determine the low-temperature activity of V-based catalysts for the SCR of NO_x with NH_3. Sci. Adv. 4 eaau4637.

Huang, H.L., Lan, Y., Shan, W.P., Qi, F.H., Xiong, S.C., Liao, Y., et al., 2014. Effect of sulfation on the selective catalytic reduction of NO with NH_3 over γ-Fe_2O_3. Catal. Lett. 144, 578–584.

Jian, Y.F., Yu, T.T., Jiang, Z.Y., Yu, Y.K., Douthwaite, M., Liu, J.Y., et al., 2019. In-depth understanding of the morphology effect of α-Fe_2O_3 on catalytic ethane destruction. ACS Appl. Mater. Interfaces 11, 11369–11383.

Leistner, K., Kumar, A., Kamasamudram, K., Olsson, L., 2018. Mechanistic study of hydrothermally aged Cu/SSZ-13 catalysts for ammonia-SCR. Catal. Today 307, 55–64.

Lian, Z.H., Shan, W.P., Wang, M., He, H., Feng, Q.C., 2019. The balance of acidity and redox capability over modified CeO_2 catalyst for the selective catalytic reduction of NO with NH_3. J. Environ. Sci. 79, 273–279.

Ma, L., Li, J.H., Fu, L.X., 2011. Catalytic performance, characterization, and mechanism study of $Fe_2(SO_4)_3$/TiO_2 catalyst for selective catalytic reduction of NO_x by ammonia. J. Phys. Chem. C 115, 7603–7612.

Ma, L., Cheng, Y.S., Cavataio, G., McCabe, R.W., Fu, L.X., Li, J.H., 2014. In situ DRIFTS and temperature-programmed technology study on NH_3-SCR of NOx over Cu-SSZ-13 and Cu-SAPO-34 catalysts. Appl. Catal. B-Environ. 156–157, 428–437.

Miszczak, S., Pietrzyk, B., 2015. Anatase-rutile transformation of TiO_2 sol-gel coatings deposited on different substrates. Ceram. Int. 41, 7461–7465.

Nova, I., dall'Acqua, L., Lietti, L., Giamello, E., Forzatti, P., 2001. Study of thermal deactivation of a de-NOx commercial catalyst. Appl. Catal. B-Environ. 35, 31–42.

Odenbrand, C.U.I., 2018. $CaSO_4$ deactivated V_2O_5-WO_3/TiO_2 SCR catalyst for a diesel power plant. Characterization and simulation of the kinetics of the SCR reactions. Appl. Catal. B-Environ. 234, 365–377.

Ramis, G., Yi, L., Busca, G., 1996. Ammonia activation over catalysts for the selective catalytic reduction of NO_x and the selective catalytic oxidation of NH_3. An FT-IR study. Catal. Today 28, 373–380.

Si, Z.C., Weng, D., Wu, X.D., Li, J., Li, G., 2010. Structure, acidity and activity of CuO_x/WO_x-ZrO_2 catalyst for selective catalytic reduction of NO by NH_3. J. Catal. 271, 43–51.

Wang, C., Yu, F., Zhu, M.Y., Tang, C.G., Zhang, K., Zhao, D., et al., 2019. Highly selective catalytic reduction of NO_x by MnO_x-CeO_2-Al_2O_3 catalysts prepared by self-propagating high-temperature synthesis. J. Environ. Sci. 75, 124–135.

Wijayanti, K., Leistner, K., Chand, S., Kumar, A., Kamasamudram, K., Currier, N.W., et al., 2016. Deactivation of Cu-SSZ-13 by SO_2 exposure under SCR conditions. Catal. Sci. Technol. 6, 2565–2579.

Woo, J.W., Bernin, D., Ahari, H., Shost, M., Zammit, M., Olsson, L., 2019. Understanding the mechanism of low temperature deactivation of Cu/SAPO-34 exposed to various amounts of water vapor in the NH_3-SCR reaction. Catal. Sci. Technol. 9, 3623–3636.

Wu, M.Z., Zhan, W.C., Guo, Y., Wang, Y.S., Guo, Y.L., Gong, X.Q., et al., 2016. Solvent-free selective oxidation of cyclohexane with molecular oxygen over manganese oxides: Effect of the calcination temperature. Chin. J. Catal. 37, 184–192.

Wu, Y.H., Chu, B.X., Zhang, M., Yi, Y.N., Dong, L.H., Fan, M.G., et al., 2019. Influence of calcination temperature on the catalytic properties of $LaCu_{0.25}Co_{0.75}O_3$ catalysts in NO_x reduction. Appl. Surf. Sci. 481, 1277–1286.

Xu, L.T., Niu, S.L., Lu, C.M., Zhang, Q., Li, J., 2018. Influence of calcination temperature on $Fe_{0.8}Mg_{0.2}O_z$ catalyst for selective catalytic reduction of NO_x with NH_3. Fuel 219, 248–258.

Yan, Z.D., Shi, X.Y., Yu, Y.B., He, H., 2019. Alkali resistance promotion of Ce-doped vanadium-titanic-based NH_3-SCR catalysts. J. Environ. Sci. 73, 155–161.

Yang, S.J., Guo, Y.F., Yan, N.Q., Wu, D.Q., He, H.P., Qu, Z., et al., 2011. Nanosized cation-deficient Fe-Ti spinel: a novel magnetic sorbent for elemental mercury capture from flue gas. ACS Appl. Mater. Interfaces 3, 209–217.

Yao, X.J., Zhao, R.D., Chen, L., Du, J., Tao, C.Y., Yang, F.M., et al., 2017. Selective catalytic reduction of NO_x by NH_3 over CeO_2 supported on TiO_2: Comparison of anatase, brookite, and rutile. Appl. Catal. B-Environ. 208, 82–93.

Ye, D., Ren, X.Y., Qu, R.Y., Liu, S.J., Zheng, C.H., Gao, X., 2019. Designing SO_2-resistant cerium-based catalyst by modifying with Fe_2O_3 for the selective catalytic reduction of NO with NH_3. Mol. Catal. 462, 10–18.

Yu, T., Wang, J., Huang, Y., Shen, M.Q., Li, W., Wang, J.Q., 2014. NH_3 oxidation mechanism over Cu/SAPO-34 catalysts prepared by different methods. ChemCatChem 6, 2074–2083.

Yu, Y.K., Miao, J.F., Wang, J.X., He, C., Chen, J.S., 2017. Facile synthesis of $CuSO_4/TiO_2$ catalysts with superior activity and SO_2 tolerance for NH_3-SCR: physicochemical properties and reaction mechanism. Catal. Sci. Technol. 7, 1590–1601.

Yu, Y.K., Chen, C.W., Ma, M.D., Douthwaite, M., He, C., Miao, J.F., et al., 2019a. SO_2 promoted in situ recovery of thermally deactivated $Fe_2(SO_4)_3/TiO_2$ NH_3-SCR catalysts: From experimental work to theoretical study. Chem. Eng. J. 361, 820–829.

Yu, Y.K., Chen, C.W., He, C., Miao, J.F., Chen, J.S., 2019b. In situ growth synthesis of CuO@Cu-MOFs core-shell materials as novel low-temperature NH_3-SCR catalysts. ChemCatChem 11, 979–984.

Zha, K.W., Kang, L., Feng, C., Han, L.P., Li, H.R., Yan, T.T., et al., 2018. Improved NO_x reduction in the presence of alkali metals by using hollandite Mn-Ti oxide promoted Cu-SAPO-34 catalysts. Environ. Sci.: Nano 5, 1408–1419.

Zhao, Y.J., Guo, Z.Y., Zhang, H.J., Peng, B., Xu, Y.X., Wang, Y., et al., 2018. Hydrogenation of diesters on copper catalyst anchored on ordered hierarchical porous silica: Pore size effect. J. Catal. 357, 223–237.